

1

Supporting Information

2

70%wt SiO₂ loaded flexible PVDF quasi-solid-state

3

electrolyte membrane for lithium oxygen battery

4 A-Qiang Wu^{a#}, Mingxing Wang^{a#}, Xiangqun Zhuge^a, Tong Liu^a, Kun Luo^{a*}, Zhihong Luo^b, Mian

5 Zhong^{c*}, Yurong Ren^a, Hanhui Lei^d, Zhanhui Yuan^e and Terence Xiaoteng Liu^{d*}

6

1. Experimental

7 *SI.1 Preparation of SiO₂ nanoparticles*

8 H₂O and NH₄OH were added in a round neck flask at a molar ratio of 7:0.5 with magnetic

9 stirring (400 rpm) for 20 min. The mixture was then heated to 25 °C and 0.17 M TEOS was added.

10 After stirring continuously for 5 h, the mixture was left overnight and then rinsed with deionized

11 water. SiO₂ nanoparticles were obtained after drying at 80 °C.

12 *SI.2 Lithium-oxygen battery assembly and testing*

13 10 mg of MWCNTs were dispersed in 30 mL of ethanol and stirred for 2 h, led to a

14 MWCNTs slurry. The slurry was sprayed evenly on 10 × 10 cm carbon paper at the loading mass

15 of 0.1 mg cm⁻², which was dried in a vacuum oven at 80 °C for 10 h, and then was cut into square

16 sheets (1 × 1 cm) as cathode of lithium oxygen battery (LOB). The assembly of coin cells

17 (CR2032, with holes in cathode side) were carried out in a glove box with argon (H₂O < 0.1 ppm,

18 O₂ < 0.1 ppm), in the sequence of "anode shell - Li plate - QSSE - glass fiber (GF, injection with

19 LiI/LiClO₄/DMSO) - cathode - cathode shell (with holes)". The LOBs were kept in the glovebox

20 overnight after sealing before testing.

21 LOBs testing were performed under pure oxygen (≥ 99.9%) atmosphere at an ambient

22 temperature (25 ± 2°C). The current density for long-term cycling was set to 1 A g⁻¹, and the

23 capacity was set to 1,000 mAh g⁻¹ (based on the loading mass of MWCNTs). The cut-off voltages

24 were set to 4.5 V and 2.0 V. In addition, the current density was set to 3, 5, and 10 A g⁻¹ for the

25 rate performance testing of the cells. For the test of full discharge capacity, the current was settled

26 as 0.1 mA and the cutoff voltage was set up to 2.0 V (Full discharge capacity = total discharge

27 time * current)/(cathode area * MWCNTs loading).

28 **SI.3 Li||Li symmetric battery assembly and testing**

29 The assembly of Li||Li symmetric battery was carried out in a glove box with high-purity
30 argon (99.999%) (H₂O < 0.1 ppm, O₂ < 0.1 ppm), in the sequence of "anode shell - stainless steel
31 (SS) gasket Li plate - QSSE - Li plate - stainless steel gasket - cathode shell". The coin cells were
32 kept in the glovebox overnight after sealing.

33 Li||Li symmetric batteries were used to study the effect of SP70 on the stability of Li anodes.
34 The applied voltage ranged from -1.5 V to 1.5 V, and the current density was 0.1 mA cm⁻², and the
35 charge/discharge time is 1 hour. The testing was carried out after standing in the argon-filled glove
36 box for 12 h.

37 Li⁺ transference number (t_{Li^+}) was measured by chronoamperometry and EIS analysis with
38 the Li||Li symmetric cells. The cell was polarized at the potential of 10 mV for 7200 s, and before
39 and after polarization the charge transfer resistance was tested by EIS. The transfer number (t_{Li^+})
40 was calculated use the following equation.

$$41 \quad t_{Li^+} = \frac{I_s(\Delta V - I_i R_i)}{I_i(\Delta V - I_s R_s)} \quad (1)$$

42 where ΔV is the polarization potential (10 mV), I_s and I_i are the initial and steady current values,
43 R_i and R_s are the charge transfer resistances before and after polarization, respectively.

44 **SI.4 SS||SS symmetric battery assembly and testing**

45 The assembly of SS||SS symmetric battery was carried out in a glove box with high-purity
46 argon (99.999%) (H₂O < 0.1 ppm, O₂ < 0.1 ppm), in the sequence of "anode shell - stainless steel
47 (SS) gasket - QSSE - stainless steel gasket - cathode shell". The coin cells were kept in the
48 glovebox overnight after sealing.

49 The Li⁺ ionic conductivity was tested by using SS||SS cells, and the EIS data was recorded by
50 an electrochemical workstation. The Li⁺ ionic conductivity (σ) was calculated according to the
51 following equation.

$$52 \quad \sigma = \frac{d}{R_b S} \quad (2)$$

53 where d is the thickness of the protective layer, R_b is the measured electric resistance, S is the
54 geometric area of the stainless steel (SS) gasket.

55 **S1.5 Electrolyte adsorption test**

56 The electrolyte adsorption rate is used to measure the adsorption capacity of the QSSEs to the
57 electrolyte. The liquid electrolyte absorption is assessed according to the below equation.

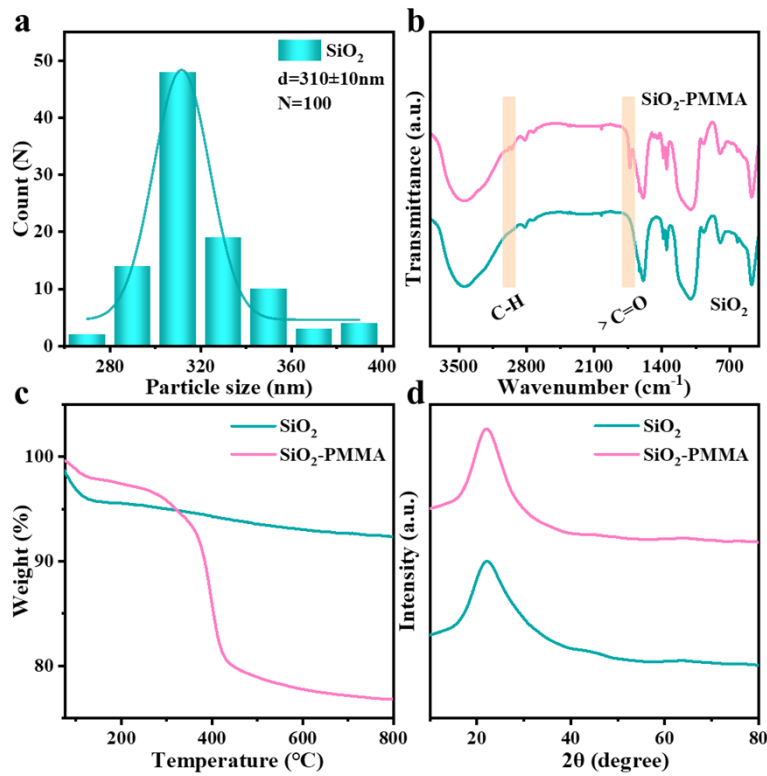
58
$$\eta = \frac{m_w - m_d}{m_d} \quad (3)$$

59 where η is the electrolyte adsorption rate, m_d and m_w represent the mass before and after
60 adsorption of the electrolyte, respectively.

61

62

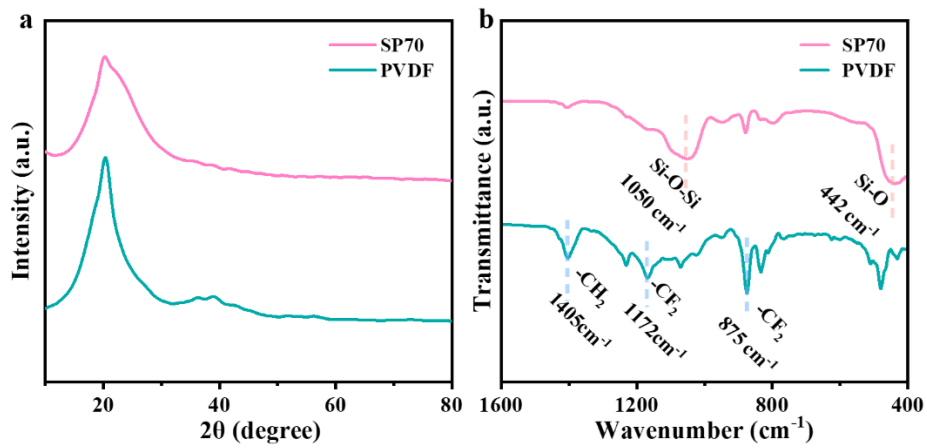
2. Supplementary Figures



63

64 **Fig. S1** Size distribution (a) of the as-synthesized SiO₂ nanoparticles; FTIR (b), TG (c) and XRD (d) analyses of
65 the SiO₂ and SiO₂-PMMA nanoparticles.

66



67

68

Fig. S2 XRD(a) and FTIR (b) analyses of the SP70 and PVDF QSSEs.

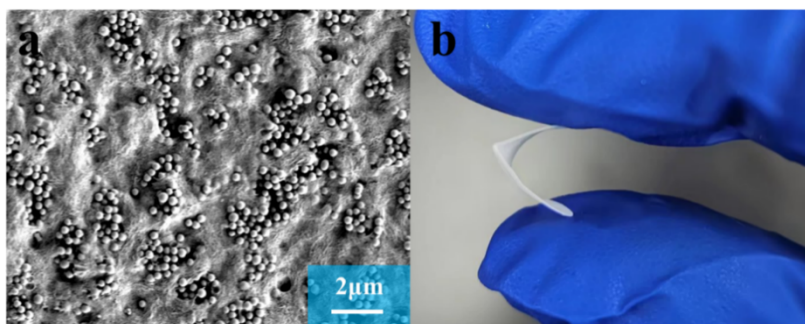
69



70

71

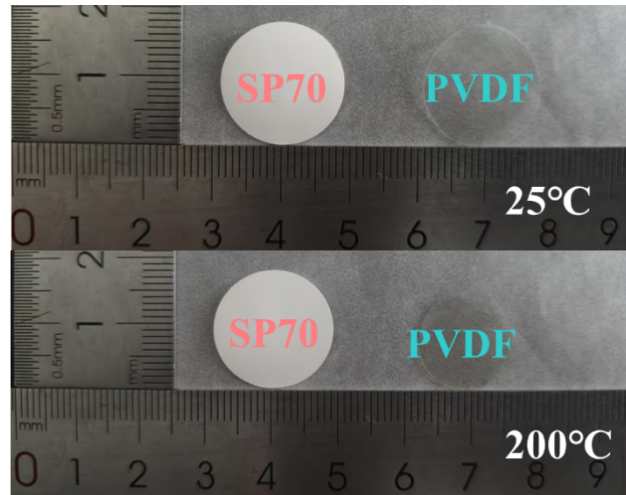
Fig. S3 Bending test of the SP80 QSSE.



72

73

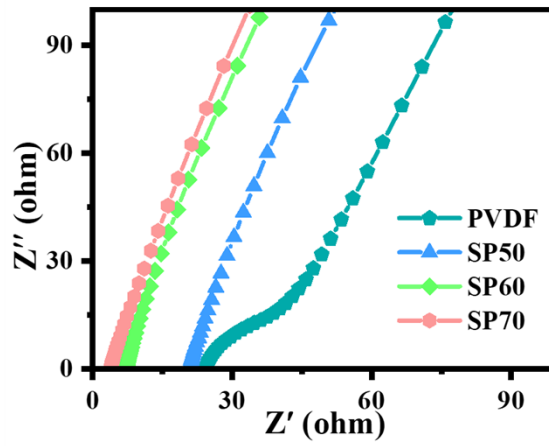
Fig. S4 SEM image (a) and bending test of the pristine SiO₂ reinforced PVDF composite.



74

75

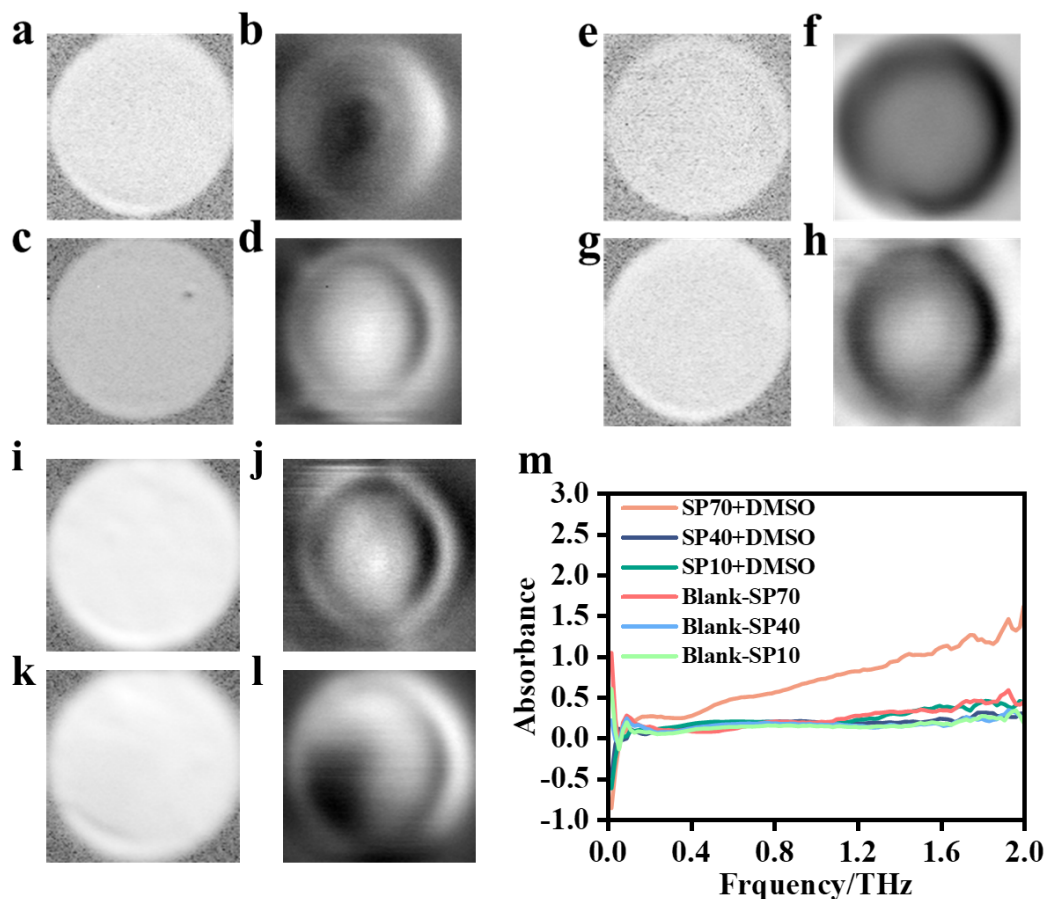
Fig. S5 Thermal stability of the SP70 and pristine PVDF QSSEs.



76

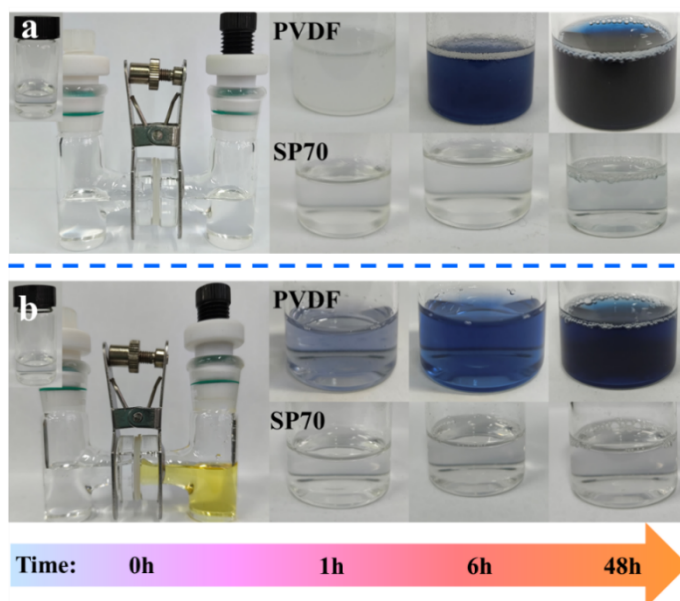
77

Fig. S6 EIS analyses of different PVDF-based QSSEs with SS||SS symmetrical cells.



78

79 **Fig. S7** Terahertz (THz) frequency-domain imaging (a) and time-domain imaging (b) of the dry SP10; THz
 80 frequency-domain imaging (c) and time-domain imaging (d) of the DMSO soaked SP10; THz frequency-domain
 81 imaging (e) and time-domain imaging (f) of the dry SP40; THz frequency-domain imaging (g) and time-domain
 82 imaging (h) of the DMSO soaked SP40; THz frequency-domain imaging (i) and time-domain imaging (j) of the
 83 dry SP70; THz frequency-domain imaging (k) and time-domain imaging (l) of the DMSO soaked SP70; THz
 84 spectra of the dry and DMSO soaked PVDF-based QSSEs (m).



85

86

Fig. S8 Permeability testing of I^- (a) and I_3^- (b) through the PVDF and SP70 QSSEs.

87

88 Permeability of the SP70 and PVDF QSSEs to iodide ions was tested using an H-type

89 electrolytic cell as follows:

90 (1) I^- permeation testing: the right column was filled with the DMSO electrolyte with 1 mol L^{-1}

91 LiClO_4 and $0.05 \text{ mol L}^{-1} \text{ LiI}$, and the left column contained $1 \text{ mol L}^{-1} \text{ LiClO}_4$ in DMSO. The two

92 columns were separated with either the SP70 or PVDF QSSE. Samples were taken from the left

93 side at different periods and tested by dropping H_2O_2 solution containing 0.5 wt.% starch (as

94 shown in the inset of **Fig.S8a** and **8b**), where the appearance of blue color indicates the crossover

95 of I^- .

96 (2) I_3^- permeation testing: the right column was filled with the DMSO electrolyte with 1 mol

97 $\text{L}^{-1} \text{ LiClO}_4$ and $0.05 \text{ mol L}^{-1} \text{ LiI}$, and the left column contained $1 \text{ mol L}^{-1} \text{ LiClO}_4$ in DMSO. The

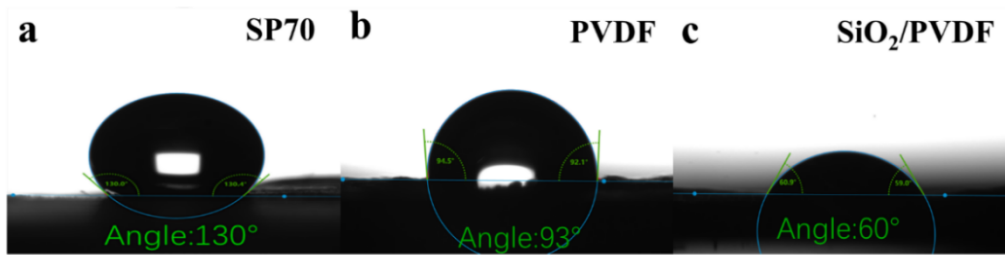
98 two columns were separated by a SP70 or PVDF QSSE. Samples were taken from the left side at

99 different periods and tested by dropping DMSO solution containing 0.5 wt.% starch (as shown in

100 the inset of **Fig.S8a** and **8b**), where the appearance of blue color indicates the crossover of I_3^- .

101

102

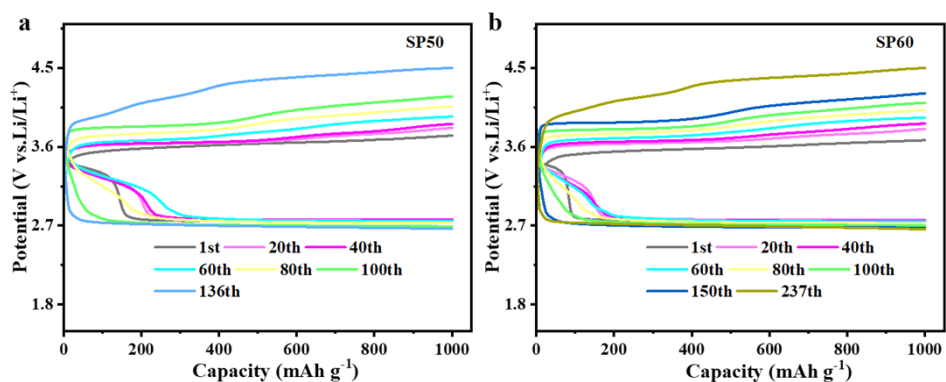


103

104 **Fig. S9** Contact angle measurement of the SP70 (a), PVDF (b) and pristine SiO₂ reinforced PVDF (c)

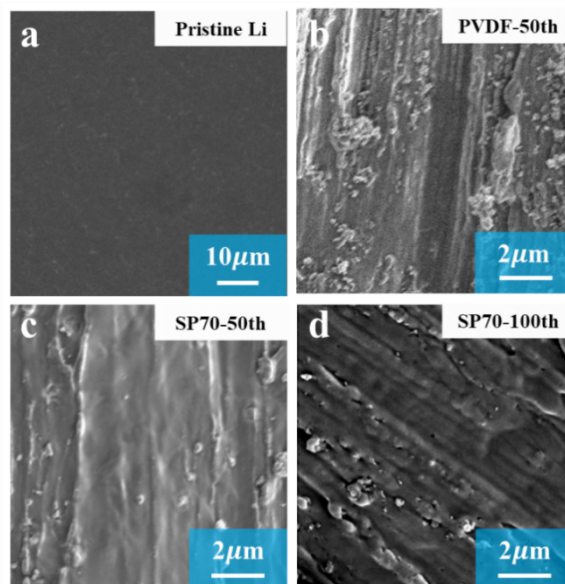
105 membranes with water drops.

106



107

108 **Fig. S10** Charge/discharge profiles in the LOBs with the SP60 (a) and SP50 (b) QSSEs.



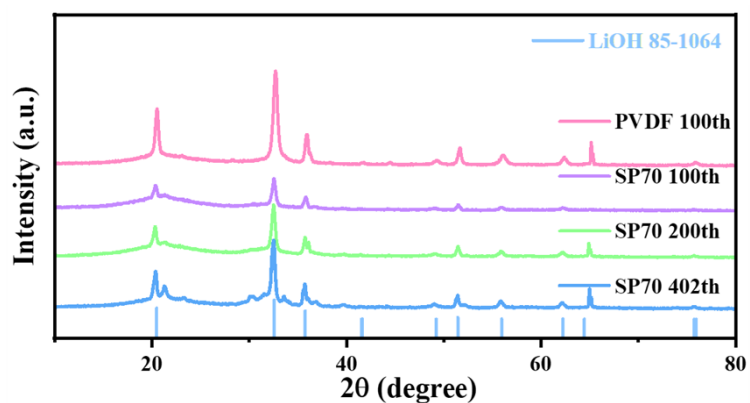
109

110 **Fig. S11** SEM images of pristine Li (a); the Li anodes with the PVDF QSSE (b) after 50 cycles and with the

111

SP70 QSSE after 50 (c) and 100 (d) cycles in the LOBs.

112

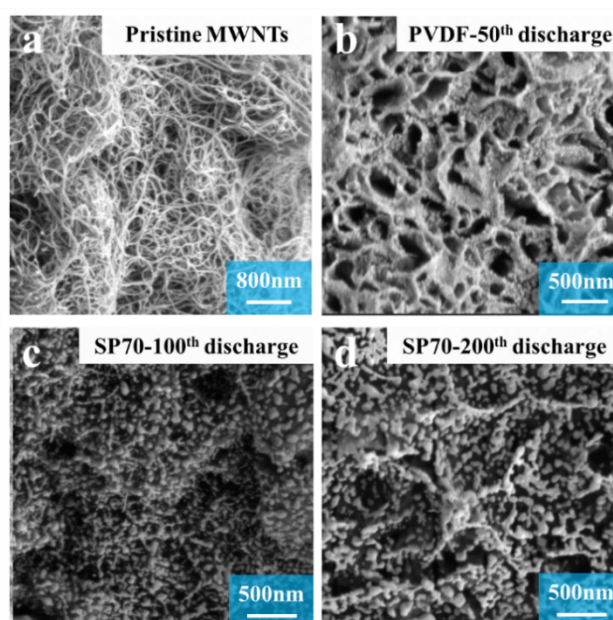


113

114 **Fig. S12** XRD analysis of the products collected from the Li anodes of LOBs with the PVDF and SP70 QSSEs

115

after different cycles.

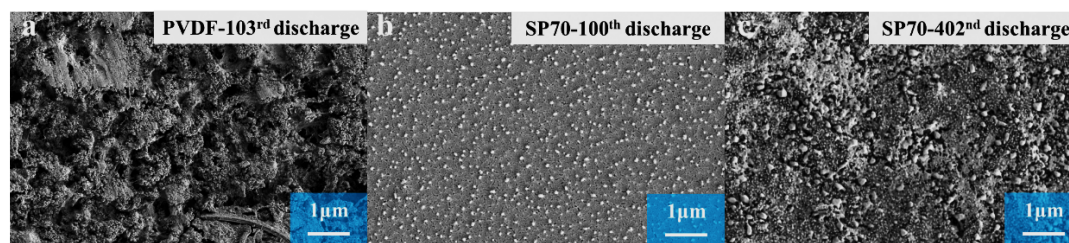


116

117 **Fig. S13** SEM images of the pristine MWCNTs (a), discharge product with the PVDF QSSE after 50 LOB cycles

118 (b), discharge product with the SP70 QSSE after 100 (c) and 200 (d) LOB cycles.

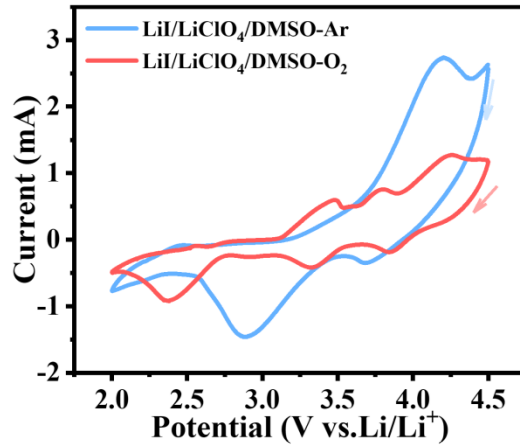
119



120

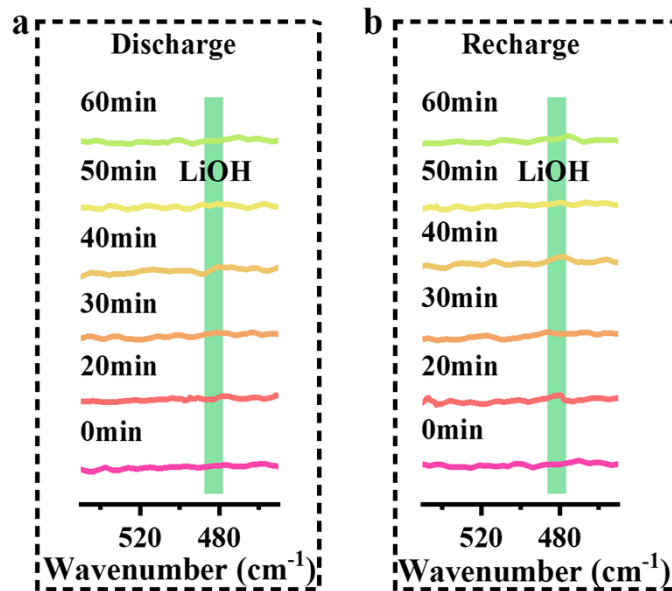
121 **Fig. S14** SEM images of the SP70 and PVDF QSSEs after different cycles at the sides toward Li anodes.

122



123

124 **Fig. S15** Cyclic voltammograms (CV) in the Li/LiClO₄/DMSO electrolyte under Ar and O₂ atmosphere.



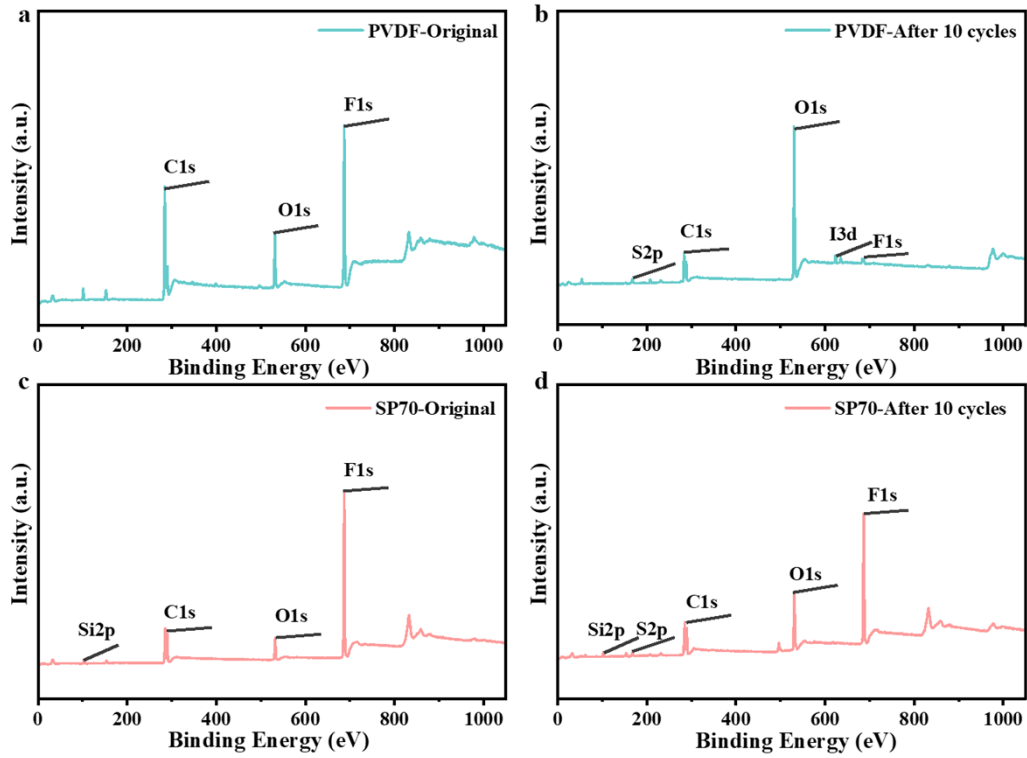
125

126 **Fig. S16** *In-situ* Raman spectroscopy in discharge (a) and recharge (b) processes at 0.3 mA cm⁻² ranging from

127

450 to 550 cm⁻¹ at the MWCNTs cathode.

128

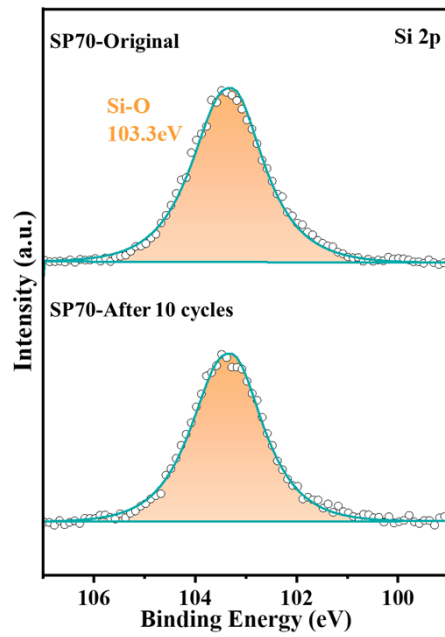


129

130 **Fig. S17** Total XPS spectra of the PVDF (a,b) and SP70 (c,d) QSSEs before and after 10 cycles at the side

131

toward Li anodes.



132

133 **Fig. S18** Fitting of the resolved Si_{2p} XPS signal of the SP70 QSSE before and after 10 LOB cycles.